

Characteristics of the Kinetic Energy Spectrum of NICAM Model Atmosphere

Koji Terasaki¹, H. L. Tanaka¹, and Masaki Satoh²

¹Center for Computational Sciences, University of Tsukuba, Tsukuba, Japan

²Center for Climate System Research, The University of Tokyo, Kashiwa, Japan

Abstract

In this study, characteristics of the energy spectrum in the zonal wavenumber domain are examined for the cloud resolving global model NICAM. A series of numerical experiments are conducted for NICAM with various horizontal resolutions from 224 km (glevel-5) to 7.0 km (glevel-10) using the T2K-Tsukuba System and 3.5 km (glevel-11) using the Earth Simulator (ES). The energy spectra of most of horizontal resolutions obey k^{-3} power law in synoptic and sub-synoptic scales (wavenumbers $k = 5$ to 30). However, the energy slope for glevel-5 becomes much steeper around zonal wavenumber $k = 10$. Nastrom et al. (1985) explained that the energy spectrum near the tropopause at wavelengths below 400 km appears to follow the $k^{-5/3}$ power. This scale corresponds to about $k = 70$ near 45°N. It is found that the energy spectra for $k > 30$ for glevel-10 and 11 follow the $k^{-5/3}$ power law. These results agree quite well with the observational studies. It is also found that the kinetic energy of the vertical wind is white noise spectrum.

1. Introduction

A new type of very high resolution atmospheric general circulation model is developed by CCSR (the Center for Climate System Research), University of Tokyo, and Frontier Research Center for Global Change/Japan Agency for Marine-Earth Science and Technology (Satoh et al. 2008). Icosahedral grid system with quasi-homogeneous grids over the sphere is used to overcome the pole problem. The model is called NICAM (Nonhydrostatic Icosahedral Atmospheric Model).

The results of the global experiments with 3.5 km horizontal mesh are reported by Tomita et al. (2005), Nasuno et al. (2007), and Miura et al. (2007). Tomita et al. (2005) succeeded in demonstrating a Madden-Julian Oscillation (MJO)-like intraseasonal oscillation, and diurnal precipitation cycles on the aqua planet experiment with glevel-10. Nasuno et al. (2007) showed that super cloud cluster propagated eastward; these have a Kelvin wave structure in dynamical fields. Miura et al. (2007) further showed that the MJO-event is realistically simulated with multi-scale structures of tropical convective systems. It is important to examine the characteristics of NICAM from various points of view for improving the new model.

The $k^{-3/3}$ power law has previously been predicted theoretically by Kolmogorov (1941) for 3D homogeneous and isotropic turbulence, producing a downscale energy flux. Using a dimensional analysis, Kraichnan

(1967) predicted the k^{-3} power law for 2D, isotropic and homogeneous turbulence in a forward enstrophy cascading inertial subrange on the short-wave side of the scale of energy injection. Nastrom et al. (1985) pointed out from the results of air-craft observations that the energy spectra of zonal wind, meridional wind, and potential temperature obey the k^{-3} power law in the synoptic scale and $k^{-5/3}$ power law in the meso scale, respectively. Koshyk and Hamilton (2001) examined the differences in the horizontal kinetic energy spectrum using the GFDL (Geophysical Fluid Dynamics Laboratory) SKYHI model with horizontal grid spacing of 35 km. They confirmed that the spectrum follows the k^{-3} power law for wavelengths between about 5000 and 500 km and $k^{-5/3}$ power law at small wavelengths. Hamilton et al. (2008) examined the horizontal spectrum of wind variance in experiments conducted with the Atmospheric GCM for the Earth Simulator (AFES), and found that the control version of AFES run at T639 horizontal spectral resolution, which employs a slightly filtered version of realistic topography, simulates a kinetic energy spectrum that compares well at large scales with global reanalyses and, at smaller scales, with available aircraft observations near the tropopause level. Tomita et al. (2008) compared the energy spectrum between AFES and NICAM glevel-7, and found that there were small differences in the lower wavenumber range.

The purpose of this study is to examine whether NICAM can reproduce the k^{-3} and $k^{-5/3}$ power spectra. In Section 2, the experimental setting and analysis method are described. In Section 3, the result of the energy spectrum in the zonal wavenumber domain is presented. Finally, the concluding remarks are given in Section 4.

2. Experimental setting and analysis method

In this study, we investigated the characteristics of the energy spectrum for NICAM from the resolution of glevel-5 to glevel-11. The model runs from glevel-5 to glevel-10 were carried out using PACS-CS (Parallel Array Computer System for Computational Sciences) and T2K-Tsukuba System, and glevel-11 using ES (Earth Simulator) (Miura et al. 2007). The corresponding horizontal resolution and analysis period are listed in Table 1. The initial data for NICAM for glevel-5 to 10 are prepared using JMA/GSM (Japan Meteorological Agency/Global Spectral Model) analysis with the resolution T319L40. The data for the first two days from the initial time are excluded from analysis as a spin-up. The cumulus parameterization of prognostic Arakawa-Schubert scheme was used for glevel-5 to glevel-8, but the cloud microphysics scheme was directly applied for glevel-9 and above. The turbulence parameterization is essential for the turbulence energy. In this study, an improved version of Mellor and Yamada level 2 with moist closure model (Nakanishi and Niino 2004; Noda et al. 2009) is used. The biharmonic horizontal diffusion is used in this study, and the diffusion coefficients are

Corresponding author: Koji Terasaki, Center for Computational Science, University of Tsukuba. 1-1-1 Tennoudai, Tsukuba, Ibaraki 305-8577, Japan. E-mail: koji@ccs.tsukuba.ac.jp. ©2009, the Meteorological Society of Japan.

Table 1. The data period used in this study for each glevel and the corresponding horizontal scale.

glevel	Δx	Analysis Period
5	224 km	2007/11/29/12Z - 2007/12/10/06Z
6	112 km	2007/11/29/12Z - 2007/12/10/06Z
7	56 km	2007/11/29/12Z - 2007/12/10/06Z
8	28 km	2007/11/29/12Z - 2007/12/03/06Z
9	14 km	2007/11/29/12Z - 2007/12/04/12Z
10	7 km	2004/06/03/00Z - 2004/06/05/18Z
11	3.5 km	2006/12/28/00Z - 2007/01/01/18Z

Table 2. The fourth-order hyperdiffusion coefficients used in this study.

glevel	hyperdiffusion coefficient ($\text{m}^4 \text{s}^{-1}$)
5	$1.000000000000 \times 10^{16}$
6	$1.250000000000 \times 10^{15}$
7	$1.562500000000 \times 10^{14}$
8	$1.953125000000 \times 10^{13}$
9	$2.019531250000 \times 10^{12}$
10	$2.524414062500 \times 10^{11}$
11	$3.155517578125 \times 10^{10}$

given in Table 2.

The terrain-following vertical coordinate ζ is adopted, which has a relation with the height z from the sea level,

$$\zeta = \frac{z_T (z - z_s)}{z_T - z_s}, \quad (1)$$

where z_T is the top of the model domain, which is set to 40 km in this study, and z_s is the height of topography.

The output data are interpolated from the icosahedral grids to equally spaced horizontal grids, and from ζ coordinate to 17 mandatory vertical levels from 1000 to 10 hPa. In this study, the energy spectrum of vertical wind speed w from 40°N to 50°N is compared first with that of zonal wind speed u and meridional wind speed v . The kinetic energy (K) is calculated as follows,

$$K(k) = \frac{1}{2} (|U_k|^2 + |V_k|^2 + |W_k|^2), \quad (2)$$

$$\approx \frac{1}{2} (|U_k|^2 + |V_k|^2), \quad (3)$$

where k is a zonal wavenumber, and U , V and W are the coefficients of Fourier transform of u , v , and w , respectively. The truncation wavenumbers of each global experiment from glevel-5 to glevel-11 are set to 80, 160, 320, 640, 1280, 2560, and 5120, respectively. As will be shown in Fig. 1, kinetic energy of the vertical component is negligible compared with that of zonal and meridional components. Therefore, the kinetic energy is evaluated using only the horizontal components.

3. Results

We first compared the kinetic energy of vertical component with that of zonal and meridional components for glevel-11 (Fig. 1). It is known that the kinetic energy spectra of the zonal and meridional components become a red noise spectrum (the energy is included mostly in large scales), and the kinetic energy of the vertical component is supposed to be a blue noise spectrum (the energy is included mostly in small scales) (Kevin Trenberth, personal communication). However, it

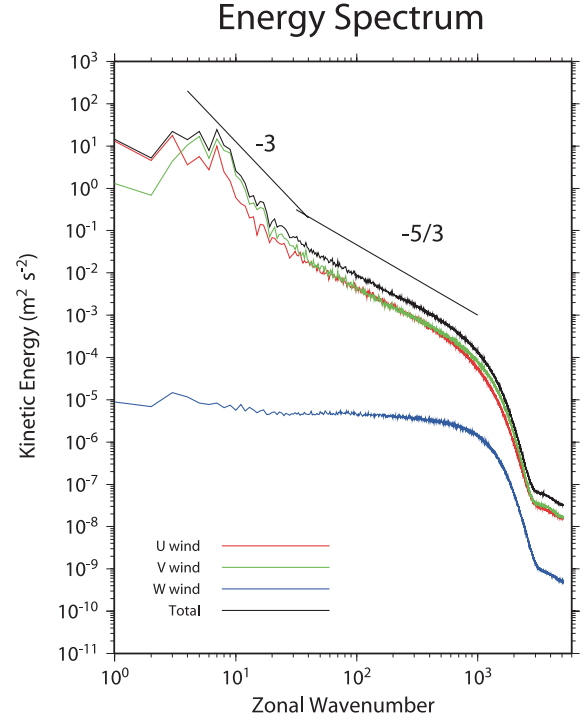


Fig. 1. The kinetic energy spectra for glevel-11 in the zonal wavenumber domain. The red, green and blue lines are the kinetic energy spectra of zonal, meridional, and vertical winds on 200 hPa surfaces from 40°N to 50°N , respectively. The total kinetic energy spectrum is drawn with black line. The k^{-3} and $k^{-5/3}$ power lines are drawn in the figure. The units are $\text{m}^2 \text{s}^{-2}$.

is found in this study that kinetic energy of the vertical component becomes a white noise spectrum, in which the vertical kinetic energy has almost the same magnitude for all wavenumbers less than 1000.

Figure 2 shows the kinetic energy spectra in the zonal wavenumber domain for glevel-5 to 11. The computed energy is averaged for whole analysis period on 200 hPa surface from 40°N to 50°N . The energy spectra of most of horizontal resolutions, except for glevel-5 and 6, obey k^{-3} power law in synoptic and sub-synoptic scales (wavenumbers $k = 6$ to 30). The energy slopes for glevel-5 and 6 become steeper than k^{-3} power around $k = 10$. The slopes of the linear regression for each glevel are listed in Table 3. The second column shows the slopes from $k = 6$ to 50, and the third column shows the slopes from $k = 70$ to 80 for glevel-5, from $k = 70$ to 100 for glevel-6, 7, and 8, from $k = 70$ to 200 for glevel-9, from $k = 70$ to 200 for glevel-10, and from $k = 70$ to 500 for glevel-11, respectively. It is expected that the energy spectrum follows the k^{-3} power for synoptic scale and $k^{-5/3}$ power for meso scales. The spectral slopes of synoptic scale for glevel-5 and 6 are -5.5559 and -4.2809 , respectively, and these are different from k^{-3} power. It would be suggested that it is difficult to represent the k^{-3} power with lower horizontal resolutions of NICAM. However, the energy spectra for the horizontal resolutions higher than glevel-7 approximately follow the k^{-3} power law.

Nastrom et al. (1985) explained with the aircraft data that the energy spectrum near the tropopause at wavelengths below 400 km appears to follow the $k^{-5/3}$ power. This scale around 45°N corresponds to about $k = 70$. It is found that experiments with lower horizontal resolutions cannot represent the $k^{-5/3}$ power spectrum (glevel-5 to 9), although the energy spectra seem to show a

similar property. In contrast, the glevel-10 and 11 can represent the $k^{-5/3}$ power spectrum, and the branch point between k^{-3} power and $k^{-5/3}$ power is near $k = 30$. There is a shift in its property between glevel-9 and 10. Horizontal grid spacing of glevel-10 is 7 km and the depth of the troposphere is about 10 km. It is suspected that these characteristics may have some effects in reproducing the feature of the 3D turbulence. The kinetic energy is dissipated by diffusion in the higher zonal wavenumbers. Therefore, the energy slope becomes steeper than $k^{-5/3}$ power, and the wavenumber where the energy drops down is different for different horizontal resolutions. The energy spectrum of glevel-10 follows the $k^{-5/3}$ power up to $k = 200$, and that of the glevel-11 follows $k^{-5/3}$ power up to $k = 500$. The energy spectrum drops down in the region of spectral tail. However, the behavior of the spectral tail depends on the numerical diffusion (Tomita et al. 2008), although the k^{-3} and $k^{-5/3}$ power laws are produced by the atmospheric dynamics (Takahashi et al. 2006).

Figure 3 shows the energy spectra in the zonal wavenumber domain for glevel-11 at the different 4 levels in the troposphere (1000, 850, 500, and 200 hPa). For comparison, the analysis result of energy spectrum by Hamilton (2008) is superimposed in the figure, which is derived from T639L24 AFES control run and aircraft data reported by Nastrom et al. (1985). The characteristics of the k^{-3} and $k^{-5/3}$ power spectra obtained in this study are consistent with the results by Hamilton (2008). The energy spectra approximately follow both k^{-3} and $k^{-5/3}$ power laws at each vertical level except for 1000 hPa surface. The energy spectrum at 1000 hPa does not follow the k^{-3} power. However, it approximately follows $k^{-5/3}$ power in the larger wavenumbers. The energy level in planetary and synoptic scales at the 1000 hPa surface is lower than that in middle and upper troposphere. But the larger energy is contained in meso scale compared to planetary and synoptic scales.

The differences in the energy spectrum on the 200 hPa level at different latitudinal circles are also shown in Fig. 4, which includes tropics (EQ–30°N), mid-latitudes (30°N–60°N), polar region (60°N–90°N), and the whole global mean. The kinetic energy of synoptic scales is the largest in the mid-latitudes, because of the existence of the tropospheric westerly jet. Spectra of all the three regions follow the k^{-3} power law. However, the spectrum of the polar region shows lower energy level at the synoptic as well as short waves and is hard to detect the $k^{-5/3}$ power spectrum. It would be suggested that the $k^{-5/3}$ power spectrum can be obtained in some restricted areas such as jet stream regions.

4. Conclusion

A new type of very high resolution atmospheric general circulation model, NICAM, is used to study the atmospheric energy spectrum.

Table 3. The slopes of kinetic energy spectrum for each glevel on 200 hPa surface. (Corresponding to the slopes of Fig. 2.)

glevel	$k = 6$ to 50	$k > 70$
5	-5.5559	-2.7188
6	-4.2809	-6.6066
7	-3.4262	-4.7915
8	-3.1725	-2.7437
9	-2.6377	-2.4662
10	-2.9524	-1.9395
11	-3.0742	-1.5192

Energy Spectrum

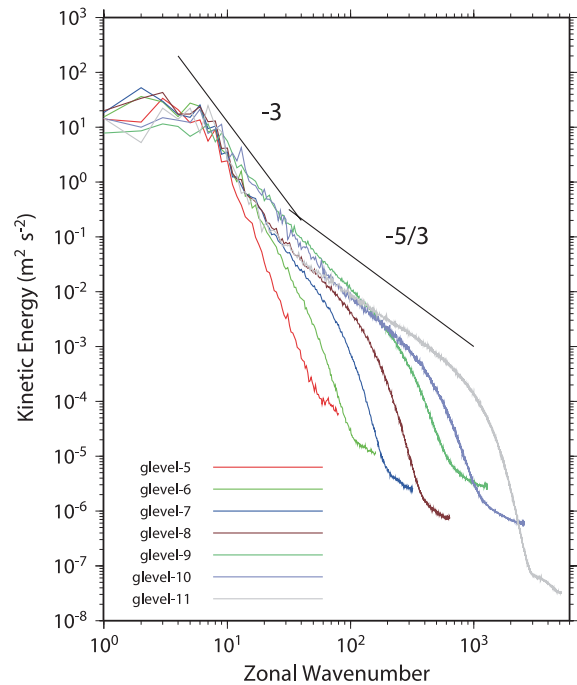


Fig. 2. The kinetic energy spectra for glevel-5 to 11 in the zonal wavenumber domain. The red, light green, blue, brown, green, light blue, and gray lines are the kinetic energy spectra on 200 hPa surface for glevel-5 to 11, respectively. The k^{-3} and $k^{-5/3}$ power lines are drawn by black lines. The units are $m^2 s^{-2}$.

NICAM is a non-hydrostatic model, so the vertical velocity is computed directly. The kinetic energy of the vertical wind component is expected to be a blue noise spectrum. However, we find that it becomes white noise spectrum. The k^{-3} and $k^{-5/3}$ power laws of kinetic energy spectrum have been studied by many researchers. In this study, the characteristics of NICAM, especially in the reproducibility of k^{-3} and $k^{-5/3}$ power laws, are analyzed in zonal wavenumber domain. We found that it is difficult to represent the k^{-3} power law with lower horizontal resolution models (glevel-5 and 6). However, the higher resolution model (glevel-7, 8, 9, 10 and 11) can reproduce the k^{-3} power spectrum.

We also found that it is difficult to reproduce the $k^{-5/3}$ power spectrum with lower horizontal resolutions (glevel-5 to 9). Since the energy spectrum by AFES shows the $k^{-5/3}$ power law with T639, it is expected that the energy spectra of NICAM for glevel-8 and 9 can reproduce the $k^{-5/3}$ power law. However, the $k^{-5/3}$ power spectrum appears only for the experiments of glevel-10 and 11. This is because NICAM is a grid-point model using the numerical diffusion, the higher-wavenumber components seem to be excessively damped compared with the spectral model (Hamilton et al. 2008). It is suggested from these results that the grid size less than 10 km is needed to reproduce $k^{-5/3}$ power spectrum for NICAM.

In this study, we focused only on the energy spectrum. It is very important to understand how the varying shapes of the energy spectra as resolution increases relate to other features of the model climate, for example, the meridional heat, vapor or momentum fluxes.

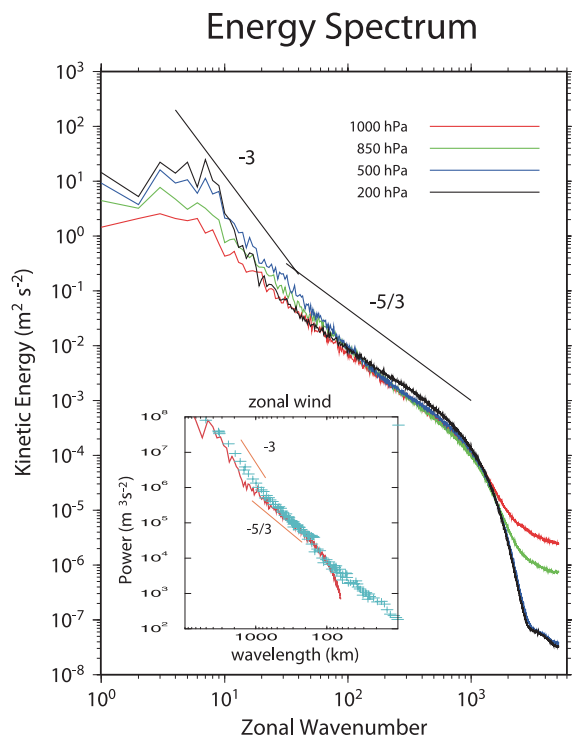


Fig. 3. The kinetic energy spectra for glevel-11 in the zonal wavenumber domain. The red, green, blue, and black lines are the energy spectra on 1000, 850, 500, and 200 hPa surfaces from 40°N to 50°N, respectively. The k^{-3} and $k^{-5/3}$ power lines are drawn by black lines. The power spectra of the aircraft data (blue + symbol) and AFES T639L24 (red line) are superimposed on this figure (cited from Hamilton 2008).

Acknowledgement

We thank Dr. H. Tomita of JAMSTEC (Japan Agency for Marine-Earth Science and Technology) for his constructive comments. The glevel-5 to 10 experiments were carried out using PACS-CS and T2K Tsukuba System. The glevel-11 experiment was conducted using the Earth Simulator. This study is partly supported by JST/CREST.

References

- Hamilton, K., Y. O. Takahashi, and W. Ohfuchi, 2008: Mesoscale spectrum of atmospheric motions investigated in a very fine resolution global general circulation model. *J. Geophys. Res.*, **113**, D18110, doi:10.1029/2008JD009785.
- Kolmogorov, A., 1941: Dissipation of energy in the locally isotropic turbulence (English translation 1991). *Proc. Roy. Soc. London*, **A434**, 15–17.
- Koshyk, J. N., and K. Hamilton, 2001: The horizontal kinetic energy spectrum and spectral budget simulated by a high-resolution troposphere-stratosphere-mesosphere GCM. *J. Atmos. Sci.*, **58**, 329–348.
- Kraichnan, R. H., 1967: Inertial ranges in two-dimensional turbulence. *Phys. Fluids*, **10**, 1417–1423.
- Miura, H., M. Satoh, T. Nasuno, T. A. Noda, and K. Oouchi, 2007: A Madden-Julian Oscillation event realistically simulated by a global cloud-resolving model. *Science*, **318**, 1763–1765.
- Nakanishi, M., and H. Niino, 2004: An improved Mellor-Yamada Level-3 model with condensation physics: its design and verification. *Boundary-Layer Meteorol.*, **112**, 1–31.

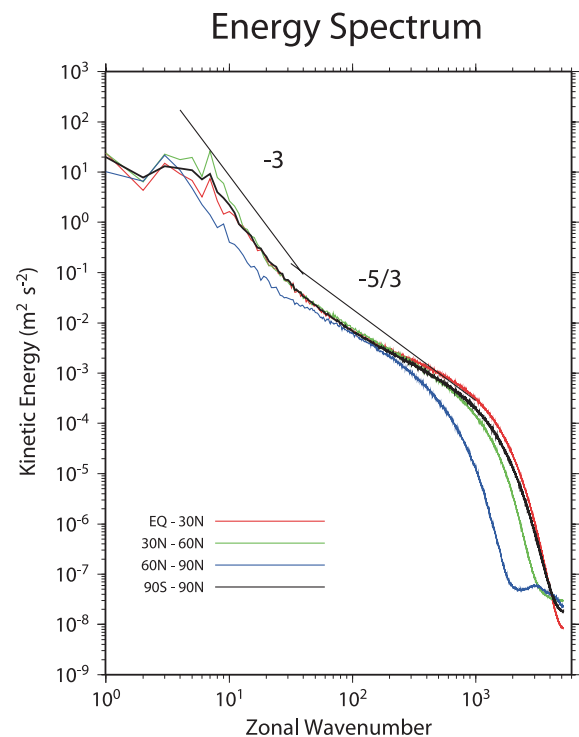


Fig. 4. The kinetic energy spectra for glevel-11 in the zonal wavenumber domain for the different latitudinal circle. The red, green, blue lines are the tropics, mid-latitudes, and polar region, respectively. The solid black line represents the global mean of kinetic energy.

- Nastrom, G. D., and K. S. Gage, 1985: A climatology of atmospheric wavenumber spectra of wind and temperature observed by commercial aircraft. *J. Atmos. Sci.*, **42**, 950–960.
- Nasuno, T., H. Tomita, S. Iga, H. Miura, and M. Satoh, 2007: Multi-scale organization of convection simulated with explicit cloud processes on an aquaplanet. *J. Atmos. Sci.*, **64**, 1902–1921.
- Noda, A. T., K. Oouchi, M. Satoh, H. Tomita, S.-I. Iga, and Y. Tsushima, 2009: Importance of the subgrid-scale turbulent moist process: cloud distribution in global cloud-resolving simulations. *Atmos. Res.*, (accepted).
- Satoh, M., H. Tomita, H. Miura, S. Iga, and T. Nasuno, 2005: Development of a global cloud resolving model – a multi-scale structure of tropical convections –, *J. Earth Simulator*, **3**, 11–19.
- Satoh, M., T. Matsuno, H. Tomita, H. Miura, T. Nasuno, and S. Iga, 2008: Nonhydrostatic Icosahedral Atmospheric Model (NICAM) for global cloud resolving simulations. *Journal of Computational Physics, the special issue on Predicting Weather, Climate and Extreme Events*, **227**, 3486–3514, doi:10.1016/j.jcp.2007.02.006.
- Takahashi, Y. O., K. Hamilton, and W. Ohfuchi, 2006: Explicit global simulation of the mesoscale spectrum of atmospheric motions. *Geophys. Res. Lett.*, **33**, L12812, doi:10.1029/2006GL026429.
- Tomita, H., H. Miura, S. Iga, T. Nasuno, and M. Satoh, 2005: A global cloud-resolving simulation: Preliminary results from an aqua planet experiment. *Geophys. Res. Lett.*, **32**, L08805, doi:10.1029/2005GL022459.
- Tomita, H., K. Goto, and M. Satoh, 2008: A new approach to atmospheric general circulation model: global cloud resolving model NICAM and its computational performance. *SIAM, J. Sci. Comput.*, **30**, 2755–2776; doi:10.1137/070692273.

Manuscript received 16 September 2009, accepted 1 December 2009
 SOLA: <http://www.jstage.jst.go.jp/browse/sola/>